Suppression of fluctuation on the angle of arrival for free-space optical communication*

LI Ming(黎明)[1,2,3]**, LIN Song**(林松)[1], **LI Shu-ming**(李书明)[1], **and YANG Shao-wen**(杨绍文)[1]

1. College of Educational Information &Technology, Hubei Normal University, Huangshi 435002, China

2. College of Physics & Electronic Information Engineering, Hubei Engineering University, Xiaogan 432000, China

3. School of Electronic Information, Wuhan University, Wuhan 430079, China

(Received 9 January 2012)

In order to increase the coupling efficiency and suppress the random angular jitter induced by atmosphere turbulent, the fine tracking system with fast steering mirror (FSM) is demonstrated. The field experiment results of free-space optical communication link across 16 km show that when there is no tracking, the range of the *x*-axis coordinates' fluctuation achieves 46 pixels, corresponding to the incident angle of 73.6 μrad, and its mean square deviation is 6.5 pixels, corresponding to the incident angle of 10.4 μrad. When there is tracking, the range of fluctuation is suppressed to 10 pixels and 16 μrad, and the mean square deviation reduces to 1.5 pixels and 2.6 μrad for the spot's centroid and the incident angle, respectively. Significantly, the coupling efficiency increases by 6 times, and the fluctuation of received light power decreases obviously.

Document code: A **Article ID:** 1673-1905(2012)04-0297-4

DOI 10.1007/s11801-012-1112-5

Free space optical (FSO) technology may become prominent in the next generation broadband networks[1,2]. The high-speed free-space optical communication links are recently being focused on. In the systems using single-mode fibers, the fiber coupling efficiency is one of the most significant issues to be solved. When a laser beam propagates through a turbulent medium like the atmosphere, the fluctuations of the angle of arrival (AOA) caused by the random deflection of the cross-section of beam can lead to the beam deviating from goal, which transforms to a spot motion or an image dancing at the focal plane of the receiver. The movement in the end face of optical fiber induces matching degree between the diffraction intensity and fiber-optic field intensity to reduce. Moreover it limits the efficiency that the laser beam is coupled into a single-mode fiber, making the received power undulate [3-5].

Adaptive optics (AO) systems can be used for correcting the aberrations induced by turbulence and for improving the coupling efficiency, but it is not a good solution because of the increased cost and the decreased receiver mobility due to using the bulkier large aperture optical elements. Furthermore, the AO system at the receiver cannot compensate for laser beam wander. If the laser beam wanders out of the receiver aperture, there will be a severe signal drop-off which causes the outage of communication system[6,7]. Another promising alternative for the fine tracking systems is to use the fast steering mirror (FSM) for suppressing the fluctuations of angle of arrival[8-10]. In Ref.[8], the design problem about the controller of FSM was addressed with the integration of an extended Kalman filter (EKF) and a linear time-invariant (LTI) single-input and single-output (SISO) system, which becomes impractical. In Ref.[9], a closed-loop fine tracking system was designed and built, but the free-space optical communication link is only 1.2 km long. Fuzzy reasoning rules were used in Ref.[10], but the suppression of the system was limited. In this paper, the efficiency for coupling space light into single-mode fiber in the presence of atmospheric turbulence is discussed, and the fine tracking system with three layers of structure back propagation (BP) neural network (NN) is demonstrated. Finally, its results of free-space optical communication link across 16 km are presented.

A uniform optical beam is focused by using a lens with the diameter of D and the focal length of f. The distribution of the optical beam on the fiber end becomes an Airy pattern, and the intensity is given by[11-13]

* This work has been supported by the Hubei Provincial Department of Education Grant (Nos.CXY2009B032 and D20102506).

** E-mail:liming 2825@126.com

$$U(r) = \exp[\mathrm{j}k(f + \frac{r^2}{2f})]\frac{\pi D^2}{4\lambda f}[2\frac{J_1(kDr/2f)}{kDr/2f}], \quad (1)$$

where k is the wave number, λ is the optical wavelength, r is the radial distance on the focal plane, and J_1 is the zero-order Bessel function of the first kind. The first zero point of the Bessel function is called the Airy disk radius ω_1. The phase term in Eq.(1) can be omitted, and it is then expressed by only the amplitude,

$$A(r) = \frac{\pi D^2}{4\lambda f}[2\frac{J_1(3.83r/\omega_1)}{3.83r/\omega_1}] \quad , \quad (2)$$

where ω_1=1.22 f/D.

The fundamental mode (LP_{01}) of power distribution in a single-mode fiber can be approximated by a Gaussian beam within 1% error[9], and it can be expressed as

$$M(r) = \sqrt{\frac{2}{\pi\omega_0}}\exp(-\frac{r^2}{\omega_0^2}) \ , \quad (3)$$

where ω_0 is the beam spot size when the amplitude is 1/e of the maximum. An offset bias ρ is defined as the static radial offset of the optical beam from the nominal axis of the fiber core. If there is an offset bias ρ, the distribution with respect to the r and ρ axes is given by the Nakagami-Rice distribution as

$$M(r,\rho) = \frac{2\sqrt{2\pi r}}{\omega_0}\exp(-\frac{r^2+\rho^2}{\omega_0^2})I_0(\frac{2r\rho}{\omega_0^2}) \ . \quad (4)$$

The angular error distribution due to the random jitter becomes a Gaussian distribution[14] with a zero mean and a variance of δ^2. When there is an offset bias error in the incident optical axis, the radial probability distribution can be given by the Rayleigh distribution as

$$p(r) = \frac{r}{\delta^2}\exp(-\frac{r^2}{2\delta^2}) \ . \quad (5)$$

Thus, the expected value of the coupling efficiency with respect to the random jitter is given by

$$\langle\eta\rangle = \frac{\left\langle|\int A(r)M(r)\mathrm{d}r|^2\right\rangle}{\left\langle\int|A(r)|^2\,\mathrm{d}r\right\rangle} = \frac{|\iint A(r)M(r,\rho)p(\rho)\mathrm{d}\rho\,\mathrm{d}r|^2}{\int|A(r)|^2\,\mathrm{d}r} . \quad (6)$$

The schematic diagram of the fine tracking system with FSM is shown in Fig.1. After receiving the beacon light, the fine tracking controller determines the angle of FSM deflection according to the coordinate of spot center in CCD, then the angle is transformed to a voltage between 0 V and 10.0 V which can drive the FSM deflection by PZT actuator. This system is possible to reduce offset bias error in the incident optical axis.

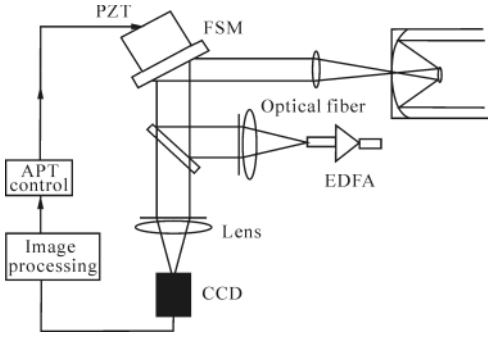

Fig.1 Schematic diagram of the fine tracking system with FSM

The artificial intelligent controller algorithm is designed by using a gain scheduled proportional-integral-differential (PID) control approach. The discrete PID controller could be written in a discrete form as

$$u(k) = u(k-1) + K_p[e(k)-e(k-1)] + K_i e(k) + K_d[e(k) -2e(k-1)+e(k-2)] , \quad (7)$$

where $e(k)$ is the desired coordinate of spot center less than actual coordinate (or error) in CCD camera, and K_p, K_i, K_d are the PID gains in Fig.2. The variable $u(k)$ is the controller output for further use in controlling PZT. It is said that NN is not only good at nonlinear approximating ability, but also fast in parallel computation, which can decrease the computing complexity. In an NN PID system, K_p, K_i and K_d are the output of NN system with respect to the error and the change of error. The problems of controlling FSM are dominated by the uncertainty of the AOA, nonlinear and lagging of FSM. In order to achieve high-precision and high-speed motion control system, the BP NN with three layers is presented for adjusting PID controller gains.

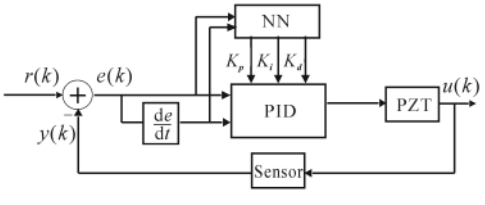

Fig.2 Schematic diagram of neuron PID control system

The BP NN in Fig.3 can be used for adjusting the gains of PID controller adaptively by using the BP method with the measurement data of $u(k)$, $y(k)$ and $r(k)$. The BP network is multilayered network which consists of an input layer, an output layer and several hidden layers of nonlinear process-

ing elements. In this paper, the BP NN with three layers is shown as Fig.3, which has the input neurons of I, the hidden neurons of J and the output neurons of P[14].

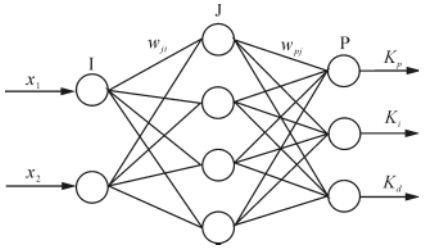

Fig.3 BP neural network with three layers

The inputs of BP neural network are

$$x_1=o_1^{\mathrm{I}}(k)=e(k),\ x_2=o_2^{\mathrm{I}}(k)=e(k)-e(k-1)\ . \tag{8}$$

The inputs and outputs of the hidden layer are

$$\begin{aligned} net_j^{\mathrm{J}}(k)&=\sum_{i=1} w_{ji}o_i^{\mathrm{I}}(k),\\ o_j^{\mathrm{J}}(k)&=f_1(net_j^{\mathrm{J}}(k)),\ (j=1,\cdots,4)\ , \end{aligned} \tag{9}$$

where net_j^{J} and o_j^{J} are the input of j-th neuron in hidden layer and the output, respectively, w_{ji} is weighting coefficient of hidden layer, $f_1(\cdot)$ is the transformation function, and $f_1(x)=(1-e^x)/(1+e^x)$.

The input and output of the output layer can be expressed as:

$$\begin{aligned} net_p^{\mathrm{P}}(k)&=\sum_{j=1}^{5} w_{pj}o_j^{\mathrm{J}}(k),\\ o_p^{\mathrm{P}}(k)&=f_2(net_p^{\mathrm{P}}(k)),\qquad (p=1,2,3),\\ K_p(k)&=o_1^{\mathrm{P}}(k),K_i(k)=o_2^{\mathrm{P}}(k),K_d(k)=o_3^{\mathrm{P}}(k), \end{aligned} \tag{10}$$

where $f_2(\cdot)$ is the activation function and $f_2(x)=e^x/(e^x+e^{-x})$.

By using the BP algorithm based on gradient method, minimize the performance index function J which can be expressed as following:

$$J=e^2(k+1)/2\ , \tag{11}$$

where J is to modify the weights by the fastest descend mean, which is searched and tuned toward the negative gradient and added on an inertia coefficient to make faster constringency.

This paper presents an experiment to examine the coupling efficiency of a laser beam propagating through atmosphere over a 16 km distance. The experiment was performed, lasting nearly one year. The laser link established between two buildings in Beijing urban is about 15 m above ground level. Landscape along the path is simple, including Guanting reservoir and several apple orchards. The receiving experimental setup is shown in Fig.4. The transmitter is a frequency-doubled Nd YAG laser with the wavelength of 1550 nm and the maximum output power of 100 mW.

The output of the Cassegrain telescope is divided into two beams by a light splitter. One of the two beams is focused on the optical fiber end face by a lens to couple space light, and the other is focused on a CCD camera by its own lens (f=200 mm) to measure the fluctuation of AOA. These devices are mounted on the 3-dimensional adjustable optics table as shown in Fig.4. The optical antenna employs the Cassegrain telescope with 2500 mm focus, where the incident angle is magnified by 50 times. The CCD camera with 16 μm pixel-pitch has sampling rate of 400 Hz. The angular resolution for a pixel-pitch is expressed by

$$\delta_{\mathrm{FOV}}=S_{\mathrm{pixel}}/f=16/(0.2\times 50)=1.6\ (\mu\mathrm{rad}). \tag{12}$$

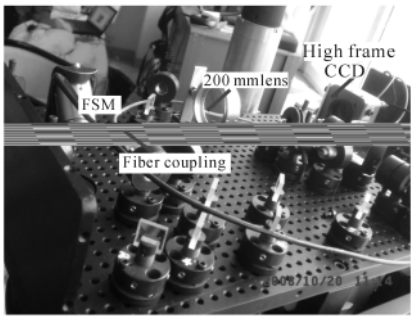

Fig.4 Photograph of the receiving experimental setup

The data set contains 8000 points sampled at 400 Hz. Fig.5 shows the histogram of spot centroid, whose distributions are similar to the normal distribution. According to the central limit theorem, a random variable which is the sum of a large number of random variables should have a normal distribution. The AOA has a linear relationship with the phase, so it should also follow a normal distribution. As the above examples presented, the horizontal turbulence (x-axis) is stronger than vertical one (y-axis). When there is no tracking, in the x-axis, the maximum range of centroid coordinates is in the region of ± 24 pixels, corresponding to the incident angle of ±38.4 μrad, and its mean square deviation is 6.5 pixels, corresponding to the incident angle of 10.4 μrad. In the y-axis, the maximum range of centroid coordinates is in the region of ±17.5 pixels, corresponding to the incident angle of±28 μrad, and its mean square deviation is 5.1 pixels, corresponding to the incident angle of 8.2 μrad. When there is tracking, in the x-axis, the range of fluctuation is suppressed to ± 5 pixels and ± 8 μrad, and the mean square deviation reduces to 1.5 pixels and 2.6 μrad for the spot's centroid and the incident angle, respectively.

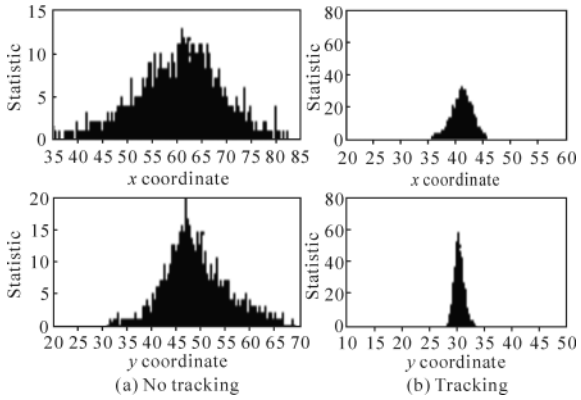

Fig.5 Statistic of AOA fluctuations

After being coupled into the optical fiber in the focal plane and amplified by erbium-doped fiber amplifier (EDFA), the received light is detected by PIN detector in Fig.1. The received optical power is measured by means of output voltage of PIN detector, which is sampled at the rate of 10000 Hz. Fig.6 shows the output voltage of PIN detector without suppressing the AOA fluctuation. The voltage fluctuates between 0.1 mV and 0.7 mV in Fig.6, which doesn't mainly exceed 0.4 mV. The results for suppressing are shown in Fig.7. The voltage fluctuates between 1 mV and 4.5 mV, which doesn't mainly exceed 4 mV. Significantly, the coupling efficiency increases by about 6 times, and the fluctuation of received light power decreases obviously.

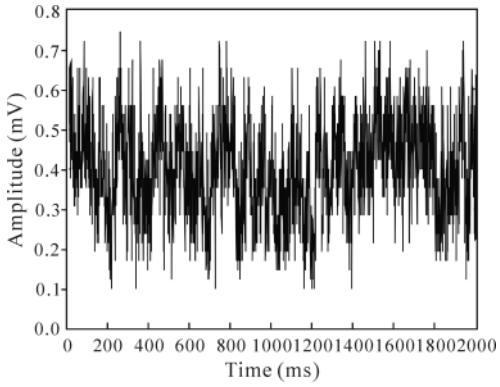

Fig.6 Acquired data of light power without tracking

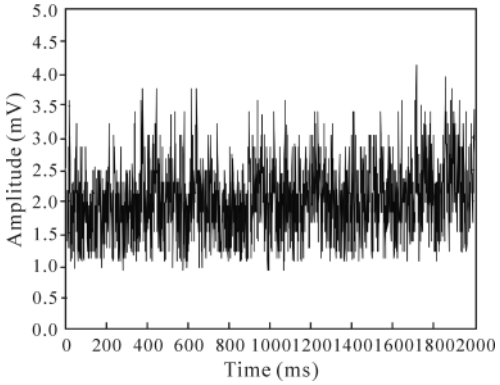

Fig.7 Acquired data of light power with tracking

In this paper, we examine the single-mode fiber coupling in FSO systems suffering from turbulence which induces the AOA fluctuations. The experimental results show that the AOA probability follows a normal distribution. The fine tracking system is demonstrated for suppressing the random angular jitter. The NN-PID controller algorithm can decrease the variance of the AOA fluctuation. Moreover the control system improves the coupling efficiency. Nowadays, such a fiber-based technology has a broad application prospect in free space optical communication. It is a precision engineering to couple the space light distorted by turbulence into the single-mode fiber.

References

[1] CAO Yang and LI Ming, Journal of Optoelectronics • Laser **21**, 683 (2010). (in Chinese)

[2] ZUO Tao, AI Yong and LI Ming, Journal of Optoelectronics • Laser **21**, 366 (2010). (in Chinese)

[3] Tarmac Dikmelik and Frederic M. Davidson, Appl. Opt. **44**, 4946 (2005).

[4] P. J. Winzer and W. R. Leeb, Opt. Lett. **23**, 986 (1998).

[5] M. L. Plett, P. R. Barbier and D. W. Rush, Appl. Opt. **40**, 327 (2001).

[6] G. A. Tyler, Journal of Optical Society of America A. **23**, 1914 (2006).

[7] J. W. Goodman, Introduction to Fourier Optics, 2nd ed., McGraw-Hill, 1996.

[8] Pérez-Arancibia Néstor O., Gibson James S. and Tsao Tsu-Chin, Laser Beam Pointing and Stabilization by Intensity Feedback Control, SPIE American Control Conference, St. Louis, 2837 (2009).

[9] Palmer K., Lotfi S. and Berglund M., IEEE J. Micromech Microengineering **20**, 1050 (2010).

[10] Cardema Jason C., Klimcak Charles M. and Herrera Alinn R., IEEE Adv. Astronaut. Sci. **140**, 1363 (2011).

[11] Wenhe DU, Liying TAN, Jing MA, Siyuan YU and Lijun JIANG, Laser and Particle Beams **28**, 90 (2010).

[12] EN Nyobe and E. Pemha, Optics Communications **283**, 1859 (2010).

[13] Babu Sena Paul, Abul Hasan, Himanshu Madheshiya and Ratnajit Bhattacharjee, IETE Journal of Research **55**, 275 (2009).

[14] S. Jaruwatanadilok and A. Ishimaru, Waves in Random and Complex Media **19**, 262 (2009).

[15] Zhang Li-Min and Guo Jin, Optics and Precision Engineering **13**, 142 (2005). (in Chinese)